Proceedings of the 2018 IEEE
International Conference on Robotics and Biomimetics
December 12-15, 2018, Kuala Lumpur, Malaysia

The characteristics of human-robot coadaptation during human-in-the-loop optimization of exoskeleton control

Wei Wang[1], Yige Liu[1], Pengqing Ren[1], Juanjuan Zhang[1] and Jingtai Liu[1], *Member, IEEE*

***Abstract*— Human-in-the-loop (HITL) optimization of exoskeleton control during assisted walking can improve human mobility and reduce the energy cost. This process involves human-robot coadaptation as suggested by prior studies. There was a drop in the same subjects metabolic cost under the same assisted walking condition before and after the optimization process. It means the subjects adapted to walking with the exoskeleton while the exoskeleton learned the optimal control parameters for the subjects. We analyzed the process of human bodies learning to walk with an ankle exoskeleton, aiming to quantify the characteristics of human-robot coadaptation during HITL optimization of exoskeleton control. Data of eleven participants from prior experiments were utilized in this study. We identified similar sample conditions for each participant and investigated the trend of metabolic cost along with the HITL exoskeleton control optimization process. Results showed that the relationship between human metabolic cost and the time past in the optimization cycle approximately followed exponential curves with widespread adaptation rates. For the optimization process of four parameters with each condition sampled for two minutes, the time constants were averaged at 238 ± 207 optimization sample conditions. Our results can provide guidance to the training process of robot assisted human motion.**

I. INTRODUCTION

Exoskeletons that can augment human strength or enhance human locomotor performance have attracted researchers for more than a century [1], [2]. As a result, in the last twenty years a couple of commercial products and laboratorial devices have achieved this goal to some extent to interact with humans and assist humans in walking or running [3]. Recently the Carnegie Mellon University developed a wearable ankle exoskeleton whose control parameters are systematically changed to maximize the performance of exoskeleton assisted human walking [4]. When humans are assisted by a robotic exoskeleton, they need to adjust themselves to learn to motion collaboratively with the exoskeleton and vice versa. Here we call this a coadaptation process. However, exoskeleton assisted human walking can be featured by nonlinear, complex and time-varying dynamics [4]. It's a challenge to quantitatively analyze the process of human-robot coadaptation during robots assisted human motion or rehabilitation.

There is a critical need to understand the characteristics of human-robot coadaptation during human-in-the-loop (HITL) optimization of exoskeleton control. Ijspeert [5] indicated that biorobotics can be used as scientific tools to investigate animal adaptive behaviors, further study the adaptive behaviors of human bodies. Felt *et al.* [6] presented instantaneous cost gradient search method to automatically identify assistive devices parameters and it was the first time that energy cost online optimization performed with the human body in the loop. Selinger [7] developed a lightweight robotic exoskeleton resisted motion of the knee joints and found that humans can optimize energy cost in real time. Jackson *et al.* [8] designed experiments to research the independent effects of net exoskeleton work and average exoskeleton torque on human locomotion and collected experimental data used to improve predictive models of human neuromuscular adaptation. Mooney *et al.* [9] analyzed the energetics and lower extremity mechanics of human walking with and without an powered ankle exoskeleton and emphasized the need for comprehensive models of human interact with exoskeleton. Koller *et al.* [10] used pneumatically actuated ankle exoskeletons to study a new type of human-robot interaction of online controller parameters optimization. Galle *et al.* [11] research the relationship between actuation timing, power and metabolic rate of powered ankle-foot exoskeletons. However, there were few researches concerning the characteristics of human-exoskeleton coadaptation during the process of HITL exoskeleton control optimization.

In this study, we investigated the process of human bodies adapting to exoskeleton assisted walking and quantified the characteristics of human-robot coadaptation of HITL optimization of exoskeleton control. Metabolic rate data and assisted control law conditions during optimization process of each participant were used from our previous experiments [4]. We constructed Importance Coefficient values for controller parameters shape the assisted torque through experiments. Moreover, by choosing the threshold values of each participant and defined relative distance of different sample assisted conditions in optimization cycle, the similar sample conditions were identified. Based on similar sample conditions, we used Nelder-Mead method to fit the metabolic cost of each participant under similar sample conditions and investigated the trend of metabolic cost along with the experienced sample conditions. We expected an exponential characteristics curve of human-exoskeleton coadaptation, as Fig.1 (a) shows. As time goes by, human bodies adaptation level increases gradually, from fast adaptation period to slow adaptation period. As a result, the metabolic cost of the human body decreased to some extent before and after the HITL exoskeleton control optimization process. Our

*This work was supported by National Natural Science Foundation (NSFC) of China under Grant 61703214 and National Natural Science Foundation of Tianjin under Grant 17JCYBJC40600.

[1]The authors are with the Institute of Robotics and Automation Information System and the Tianjin Key Laboratory of Intelligent Robotics, Nankai University, Tianjin 300071, China. Corresponding author's e-mail: juanjuanzhang@nankai.edu.cn

978-1-7281-0377-8/18/$31.00 ©

study may to some extent provide an intuitive understanding of the characteristics of human-robot coadaptation during exoskeletons assisted walking.

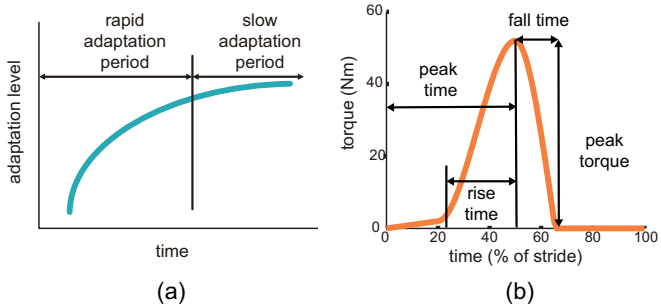

Fig. 1. (a) The characteristics between a human's adaptation level and adaptation time. (b) Parameterization of ankle torque.

II. METHOD

A. Experimental Setup

A tethered, torque-controlled 1-DoF wearable ankle exoskeleton emulator was used as a platform to conduct our research [4]. Platform structure can be seen from Fig. 2. The exoskeleton emulator was composed of three main modules: an off-board control module, a transmission module and an ankle exoskeleton. The off-board control module was comprised of a high-speed control system (ACE1103, dSPACE) and an electric motor (BSM90N-175AD, Baldor Electric). The transmission module was composed of a uni-directional Bowden cable transmission with a series leaf spring. Series-elastic transmission can improve torque tracking performance and is safety in human-exoskeleton interaction [12], [13]. The ankle exoskeleton was constructed mainly by a carbon fiber exoskeleton frame and a digital optical encoder (E8P, US Digital) that measured ankle joint angular. The structure of ankle exoskeleton used in the system was described in detail in [14].

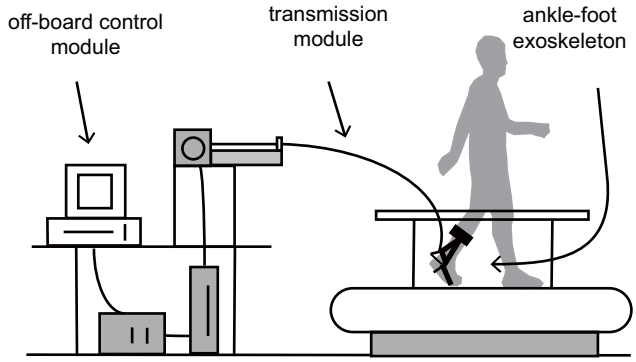

Fig. 2. Structure of the exoskeleton emulator platform.

Each control law condition determined the applied exoskeleton ankle torque as a function of time, normalized to stride period. It has a hill-like shape as shown in Fig.1 (b). As shown in Fig.1 (b), four primary parameters were selected to define the ankle torque curve: peak torque τ_p, peak torque time t_p, rise time t_r, and fall time t_f. Peak time t_p represents the beginning of a stride to the peak ankle torque time; rise time t_r represents the onset time to the peak ankle torque time; peak torque τ_p represents the maximum ankle torque value; fall time t_f represents the peak torque time to the zero torque point.

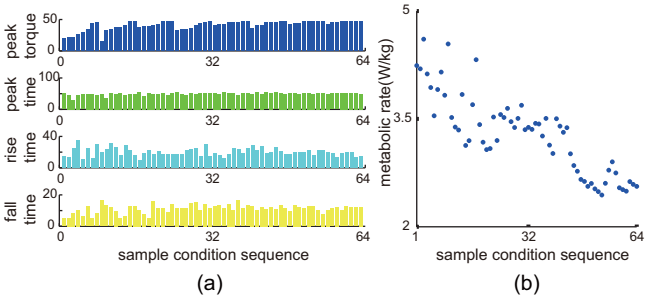

Fig. 3. (a) P1's 64 sample conditions parameters during exoskeleton assisted walking. (b) P1's metabolic rate data over 64 sample conditions.

A Covariance Matrix Adaption Evolution Strategy (CMA-ES) was used to optimize the exoskeleton control parameters which can minimize the metabolic energy cost during walking for each participant. CMA-ES fits for non-linear, non-convex and noisy optimizing problems [15]. We chose a population size of eight exoskeleton control laws for each generation. For each participant, from previous experiments [4], we optimized four generations. Most participants optimized another four generations in addition to test whether the optimization had converged. For example, Fig. 3 (a) shows P1's 64 sample conditions parameters during exoskeleton assisted walking. Estimated metabolic rate which we mentioned in the following paragraphs was used as the objective function of HITL exoskeleton control optimization. An overview of the algorithm is presented as pseudo-code in proceeding sections.

According to [16] and previous experiments [4], each sample condition needs two minutes walking to estimate the metabolic rate. Breath-by-breath rates of O_2 consumption and CO_2 production were collected through wireless portable respirometry system (Oxycon Mobile; CareFusion). Then method in [16], [17] was used to estimate the real-time metabolic rate. Fig. 3 (b) takes P1's metabolic rate during 64 exoskeleton sample conditions for example.

Eleven healthy subjects (N = 11, 5 female and 6 male; age = 27 ± 4.2 $[24-37]$ years; body mass = 69.6 ± 14.1 $[50-93]$ kg; height = 1.75 ± 0.10 m; mean±standard deviation [range];) provided written informed consent and participated in this study. Participants details can be seen in Table I.

B. Normalization

From previous experiments [4], we introduced limits to constraint the four control parameters. The first parameter of peak torque's maximum value is restricted in 1 N.m.kg^{-1}, which is one Newton meter for each kilogram of subject's body mass. Peak torque time is constrained to between 10% and 55% of stride. Rise time is restricted to between 10%

Algorithm 1 Human-in-the-loop optimization of exoskeleton control using CMA-ES

Require: Number of optimization variables N, step size σ, stop fitness ϵ, initial means of optimization variables $\boldsymbol{m}$.

Initialize intermediate parameters λ, μ, ω_i, c_σ, d_σ, μ_{cov}, c_{cov} to default values, set evolution paths $\boldsymbol{p_\sigma} = 0$, $\boldsymbol{p_c} = 0$ and set covariance matrix $\boldsymbol{C} = \boldsymbol{I}$.
while Not meet termination criterion **do**
  Generate λ offsprings contained control parameters τ_p, t_p, t_r, t_f
  Evaluate metabolic cost as objective function of each offspring of control parameters
  Sort by metabolic costs and compute weighted mean into $\boldsymbol{m}$
  Cumulation: Update evolution paths $\boldsymbol{p_\sigma}, \boldsymbol{p_c}$
  Adapt covariance matrix $\boldsymbol{C}$ and step size σ
  Decomposition of $\boldsymbol{C} = \boldsymbol{B}\boldsymbol{D}^2\boldsymbol{B}^T$
  Break, if exceed max iterations or meet stop fitness
end while
return

TABLE I
PARTICIPANTS DETAILS

Participant	Gender	Body mass (kg)	Exoskeleton Experience
P1	F	57	NO
P2	M	80	YES
P3	F	50	NO
P4	M	83	NO
P5	M	86	YES
P6	M	70	NO
P7	F	68	YES
P8	F	59	YES
P9	F	55	YES
P10	M	65	NO
P11	M	93	NO

and 40% of stride time. At last, fall time is constrained to between 5% and 20% of the stride period.

Control parameters normalization can be calculated by Equ.(1).

$$\begin{aligned} \overline{p}_1 &= \frac{p_1}{subject\_weight} \\ \overline{p}_2 &= \frac{p_2 - 10}{55 - 10} \\ \overline{p}_3 &= \frac{p_3 - 10}{40 - 10} \\ \overline{p}_4 &= \frac{p_4 - 5}{20 - 5} \end{aligned} \tag{1}$$

where p_i represents original control parameters; $\overline{p}_i (i = 1, 2, 3, 4)$ represents normalized control parameters. The mean and standard deviation of all participants' four parameters after normalization are shown in Fig. 4 (b).

C. Identifying Similar Sample Conditions

Because there are no strictly identical sample assist conditions in our experiment, we need to select a variety groups of similar conditions for each participant. A weighted distance between different conditions and same threshold values in four control parameters are used to selected similar conditions from each participant's all sample conditions. We iterate all conditions of each subject, then take the current condition in each iteration as reference condition and use Equ. (2) to select conditions are similar to reference condition. In order to increase the accuracy of characteristic curves fitting results of human-exoskeleton coadaptation, at least eight conditions are contained in a similar conditions group.

$$w_i |\overline{p}_{ij} - \overline{p}_{ri}| \leq \epsilon \tag{2}$$

where w_i is the weight of each control parameter, $i = 1, 2, 3, 4$ refers to i^{th} parameter; $\overline{p}_{ij}$ is the j^{th} condition of parameter i of each participant; $\overline{p}_{ri}$ is the reference condition of parameter i in current iteration; ϵ is the threshold value of each control parameter, and the four control parameters' threshold values of each participant are the same.

Weight value of each control parameter is defined by optimized control law parameter values of all participants. The range of optimized control parameters of all participants can be seen in Fig. 4 (a).

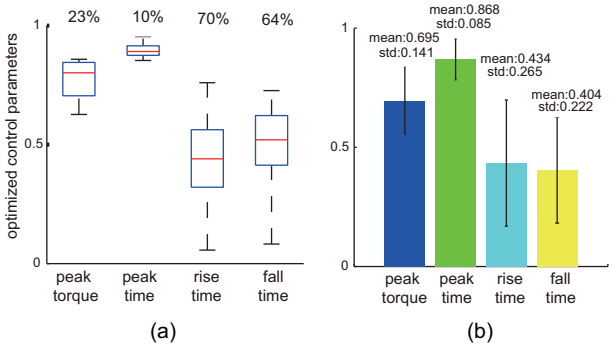

Fig. 4. (a) Range of optimized control law parameters of all participants. (b) Averaged mean and standard deviation of all participants sample conditions after normalization.

[11] indicated that assistance actuation timing and exoskeleton power have a great influence on metabolic cost during walking. Meanwhile, previous experiment [4] suggested that the parameters of peak torque and peak time had a greater influence on metabolic cost during walking than other parameters. So we introduce Importance Coefficient (ImpC) to represent the importance of each parameter. ImpC of each parameter is calculated by the following equation:

$$r_i = \frac{1}{range_i} \tag{3}$$

where i represents the i^{th} parameter; $range_i$ is the optimized range value of i^{th} parameter in Fig. 4 (a). The value of ImpC of each parameter can be seen in Table II.

Weight value of each parameter depends on ImpC. We scale the ImpC and let the sum of weight values equal to one to achieve final weight value of each parameter. The weight value of each parameter can be seen in Table III. Weight values also can reflect the importance of each parameter.

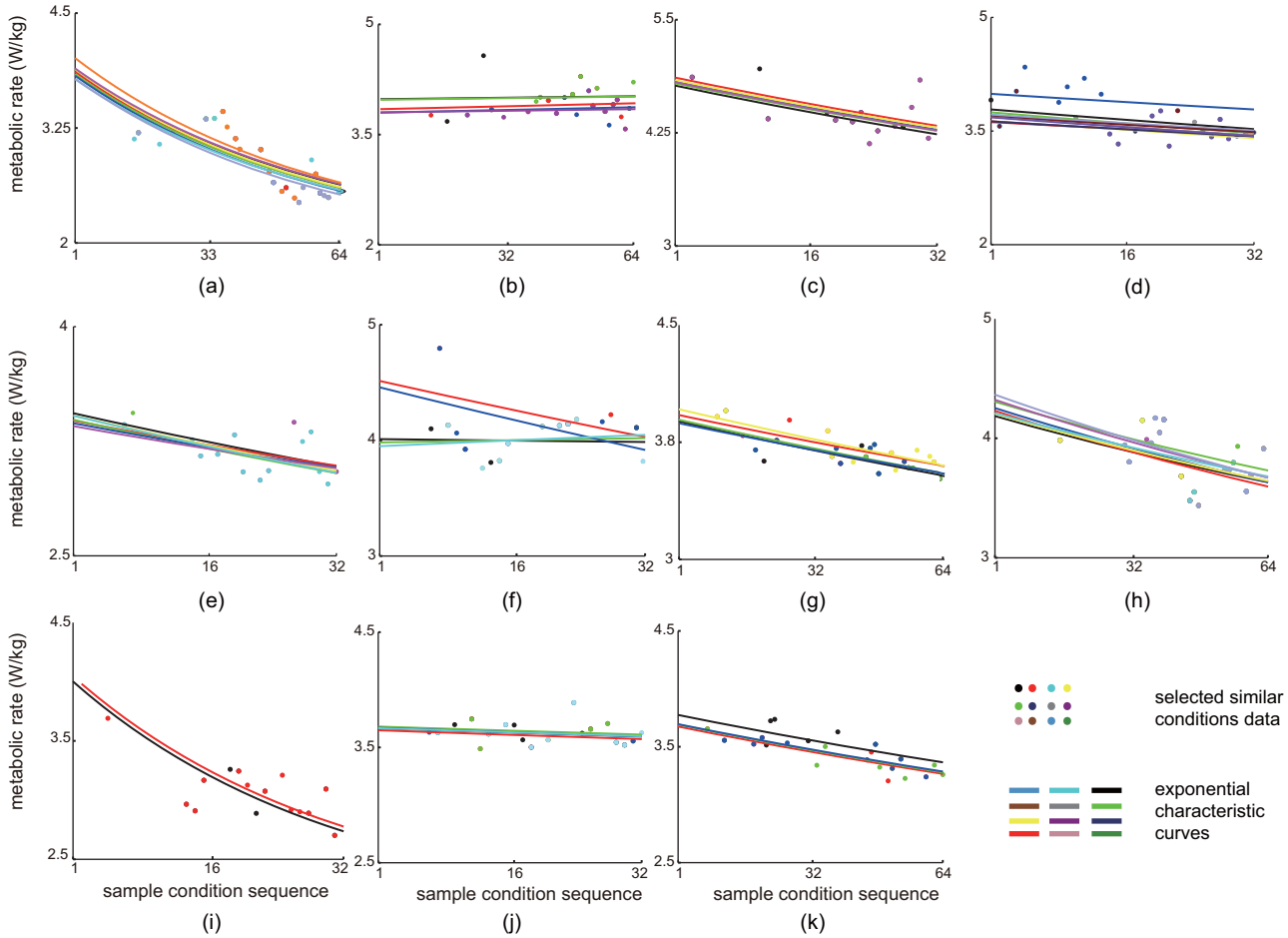

Fig. 5. All participants selected similar sample conditions and characteristic curves of human-robot coadaptation.

TABLE II
IMPORTANCE COEFFICIENT VALUE OF EACH PARAMETER

r_1	r_2	r_3	r_4
4.35	10	1.43	1.56

TABLE III
WEIGHT VALUE OF EACH PARAMETER

w_1	w_2	w_3	w_4
0.25	0.58	0.08	0.09

D. Characteristic Curve Fitting of Similar Sample Conditions

Nelder-Mead method is used to minimize objective function aiming to fit the metabolic cost of each participant under similar sample conditions. Nelder-Mead method is a heuristic search method commonly used to solve nonlinear optimization problem [18]. We expected an exponential effect of experienced sample conditions on metabolic energy cost of each participant. We use the following Equ. (4) to fit the selected similar sample conditions of each participant.

$$f_{\text{metaR}}(n)_i^k = a_i + b_i e^{-\frac{n}{\tau}} \tag{4}$$

where k represents the k^{th} participant; a_i, b_i are exponential curve fitting parameters of the i^{th} condition; τ represents the time constant of one participant. For one certain participant, different exponential curve fittings have the same time constant τ.

RMSE between curve fitting values and real metabolic rates are selected as the objective function:

$$G_k = \sqrt{\sum_{i=1}^{N}[(a_i + b_i e^{-\frac{t(i)}{\tau_k}}) - real(t(i))]^2} \tag{5}$$

where N is the quantity of each participant selected fixed conditions; a_i, b_i, τ_k are exponential curve fitting parameters to be optimized; k represents the k^{th} participant and i represents the i^{th} fixed condition of each participant; $t(i)$ is the i^{th} condition's moment.

RMSE and Coefficients of determination (R^2) are calculated to evaluate how well the characteristic curves match with the selected similar conditions.

TABLE IV
DIFFERENT CURVE FITTING RESULTS OF HUMAN-ROBOT COADAPTATION

Participant	Exponential curves		Linear curves		Power curves	
	RMSE	R^2	RMSE	R^2	RMSE	R^2
P1	0.636	0.80	0.579	0.83	0.825	0.73
P2	0.543	0.07	0.543	0.07	0.541	0.12
P3	0.585	0.60	0.590	0.59	0.551	0.65
P4	0.478	0.27	0.515	0.27	0.484	0.28
P5	0.355	0.55	0.357	0.54	0.349	0.58
P6	0.524	0.27	0.560	0.20	0.521	0.17
P7	0.214	0.75	0.216	0.75	0.212	0.73
P8	0.686	0.49	0.687	0.49	0.702	0.48
P9	0.738	0.82	0.809	0.77	0.677	0.88
P10	0.303	0.21	0.303	0.21	0.303	0.20
P11	0.231	0.81	0.229	0.82	0.258	0.75
	0.481	0.513	0.490	0.504	0.493	0.501

III. RESULTS

Based on CMA-ES optimizing four parameters of each sample condition, participants walked 32 to 64 powered exoskeleton sample conditions. Each sample condition needs 2 minutes' walk to estimate the metabolic rate. There was no rest between two sample conditions. Because of physical limitations, participants would have a rest after 32 sample conditions. Because P2 has a significant difference in characteristic curves and time constant from other participants, so we statistically analyze all participants results except P2.

As shown in Fig.5 (a)-(k), there was a drop in the same participant's metabolic cost under the same assisted walking condition before and after the HITL exoskeleton control optimization process. The relationship between participants' metabolic cost and the time past in the optimization cycle approximately follows exponential curves. However, the time constants τ of all participants are different. Time constants range from 31 to 769 (experienced sample conditions), and with an averaged value of 238 ± 207 sample conditions. P1 and P9 have relatively small time constants, which are 59 and 31 when using 64 and 32 sample conditions, respectively. According to human-robot coadaptation characteristic curves of each participant, metabolic cost decreased with an average value of $13.15 \pm 10.59\%$ and range from 1.96% to 32.73% before and after the optimization process. Human-robot coadaptation characteristic curves details for different participants are shown in Table V.

More in detail, we compare the exponential characteristic curves with linear characteristic curves and power characteristic curves to illustrate the human-robot coadaptation process of walking follow exponential downward trend. Linear and power characteristic curves results are shown in Table IV. For each participant, the threshold value ϵ and selected similar conditions groups among exponential characteristic curves and other characteristic curves are the same, which can be seen in Table V. Averaged RMSE of exponential characteristic curves is 0.481, 1.73% lower than linear characteristic curves whose averaged RMSE is 0.490, and 2.37% lower than power characteristic curves whose averaged RMSE is 0.493. Averaged R^2 of exponential characteristic curves is 0.513, 1.81% greater than linear characteristic curves whose averaged R^2 is 0.504, and 2.34% greater than power characteristic curves whose averaged R^2 is 0.501.

IV. DISCUSSION

The overall goal of our study is to quantitatively analyze the characteristics of human-robot coadaptation of HITL optimization of exoskeleton control. As shown in our results, the RMSE and R^2 of exponential characteristic curves are better than linear characteristic curves and power characteristic curves. Results demonstrate the process of human-robot coadaptation of a HITL optimization of exoskeleton control in accordance with exponential characteristic curves.

From our characteristic curves shown in Fig. 5 (a) and (f), the metabolic rate of P1 and P9 decreased exponentially before and after the optimization process. It also means they have a faster adaptation rate than other participants. This phenomenon in line with what we found in the experiments. In previous experiments, though there was no prior experience in using exoskeleton, P1 adapted quickly to walking with the ankle exoskeleton. The body of P9 was already tired before the experiment, therefore exoskeleton assistance was importance when P9 used exoskeleton to assist walking.

From Fig.5 (b), the metabolic cost of P2 along with the optimization process increased slightly. Because P2 had extensive experience in using exoskeleton, he might not increase the human-robot coadaptation level of the HITL exoskeleton control optimization process. This is why the metabolic rate of P2 remained steady or even increased slightly during the process. In the future, we plan to conduct more experiments to research the human-robot coadaptation characteristics of extensive experienced human bodies.

P3, P4 and P5 experienced 64 sample consitions in the HITL exoskeleton control optimization process and we selected front 32 sample conditions because the latter 33-64 sample conditions contained strong noise. Moreover, the participants experienced physical fatigue that could affect their characteristic curves. From Fig.5 (c), (d) and (e), these three participants have moderate adaptation rates. The time constants of P3-P5 are greater than P1 and P9, but smaller than P7 and P10.

P6 and P10 also experienced 64 sample conditions and we selected latter 33-64 sample conditions because the front 1-33 sample conditions have pauses in the experiment due to equipment failures or algorithm errors. Fig.5 (f) and (j) show that two participants have slower adaptation rates. Especially for P10, whose time constant is the greatest of all participants. This phenomenon is in accordance with previous optimization experiments. In the experiments, P6 and P10 adapted to walking with the exoskeleton for a long time.

P7 experienced 64 sample conditions in total. Fig.5 (g) shows that P7 have a relatively slower adaptation rate. This is also in line with our previous experiments. In the future, we

TABLE V

EXPONENTIAL CHARACTERISTIC CURVES OF HUMAN-ROBOT COADAPTATION FOR EACH PARTICIPANT

Participant	Threshold ϵ	Selected Groups	Time Constant τ	Prior Exoskeleton Experience	RMSE	R^2	Sample Condition Sequence
P1	0.015	9	59	NO	0.636	0.80	$1-64$
P2	0.020	5	-2000	YES	0.543	0.07	$1-64$
P3	0.030	6	128	NO	0.585	0.60	$1-32$
P4	0.040	13	238	NO	0.478	0.27	$1-32$
P5	0.035	7	147	YES	0.355	0.55	$1-32$
P6	0.030	5	256	NO	0.524	0.27	$1-32$
P7	0.025	5	312	YES	0.214	0.75	$1-64$
P8	0.018	8	192	YES	0.686	0.49	$1-64$
P9	0.045	2	31	YES	0.738	0.82	$1-64$
P10	0.025	5	769	NO	0.303	0.21	$1-32$
P11	0.014	4	250	NO	0.231	0.81	$1-64$

plan to study the reason why P7 have a slower adaptation rate although this participant had experience in using exoskeleton.

P8 and P11 all experienced 64 sample conditions. From Fig.5 (h) and (k), these two participants have moderate adaptation rates like P3-P5. This is also in line with our previous experiments.

V. CONCLUSIONS

Using HITL optimization method, a human body walking with an assisted exoskeleton is a human-robot coadaptation process. Exoskeleton optimized control parameters to reduce the metabolic rate during human walking. At the same time, the human body adjusted themselves to adapt to the exoskeleton. In this study, we analyzed the process of human bodies learning to walk with an exoskeleton and quantified the characteristics of human-robot coadaptation during a HITL exoskeleton control optimization process. Results from our study demonstrated that the process of human-robot coadaptation conforms to exponential curves, subject's metabolic rate decreased exponentially during exoskeleton control optimization process. Moreover, for the optimization process of four parameters with each condition sampled two minutes, the time constant of eleven participants were averaged at 238 ± 207 optimization sample conditions. The results may to some extent provide an intuitive understanding of the characteristics of human-robot coadaptation during exoskeletons assisted walking and are helpful for guiding the training process of robot assisted human motion.

As a future work, we plan to conduct experiments include more participants to validate the exponential characteristics curve of human-robot coadaptation, and further research the human-robot coadaptation characteristics between experienced and inexperienced participants. Moreover, as our previous system concerned more on unilateral exoskeleton assistance, we expect to improve our system to study the human-robot coadaptation characteristics in bilateral exoskeleton assistance situation.

ACKNOWLEDGMENT

This research was supported by National Natural Science Foundation (NSFC) of China under Grant 61703214 and National Natural Science Foundation of Tianjin under Grant 17JCYBJC40600.

REFERENCES

[1] Warren Cornwall. In pursuit of the perfect power suit. *Science*, 350(6258):270–273, 2015.

[2] Luke M Mooney, Elliott J Rouse, and Hugh M Herr. Autonomous exoskeleton reduces metabolic cost of human walking. *Journal of neuroengineering and rehabilitation*, 11(1):151, 2014.

[3] Erico Guizzo and Harry Goldstein. The rise of the body bots [robotic exoskeletons]. *IEEE spectrum*, 42(10):50–56, 2005.

[4] Juanjuan Zhang, Pieter Fiers, Kirby A Witte, Rachel W Jackson, Katherine L Poggensee, Christopher G Atkeson, and Steven H Collins. Human-in-the-loop optimization of exoskeleton assistance during walking. *Science*, 356(6344):1280–1284, 2017.

[5] Auke J Ijspeert. Biorobotics: Using robots to emulate and investigate agile locomotion. *Science*, 346(6206):196–203, 2014.

[6] Wyatt Felt, Jessica C Selinger, J Maxwell Donelan, and C David Remy. "body-in-the-loop": Optimizing device parameters using measures of instantaneous energetic cost. *PloS one*, 10(8):e0135342, 2015.

[7] Jessica C Selinger, Shawn M OConnor, Jeremy D Wong, and J Maxwell Donelan. Humans can continuously optimize energetic cost during walking. *Current Biology*, 25(18):2452–2456, 2015.

[8] R. W. Jackson and S. H. Collins. An experimental comparison of the relative benefits of work and torque assistance in ankle exoskeletons. *Journal of Applied Physiology*, 119(5):541–57, 2015.

[9] Luke M. Mooney and Hugh M. Herr. Biomechanical walking mechanisms underlying the metabolic reduction caused by an autonomous exoskeleton. *Journal of Neuroengineering and Rehabilitation*, 13(1):1–12, 2016.

[10] Jeffrey R Koller, Deanna H Gates, Daniel P Ferris, and C David Remy. 'body-in-the-loop'optimization of assistive robotic devices: A validation study. In *Robotics: Science and Systems*, 2016.

[11] Samuel Galle, Philippe Malcolm, Steven Hartley Collins, and Dirk De Clercq. Reducing the metabolic cost of walking with an ankle exoskeleton: interaction between actuation timing and power. *Journal of neuroengineering and rehabilitation*, 14(1):35, 2017.

[12] Gill A Pratt and Matthew M Williamson. Series elastic actuators. In *Intelligent Robots and Systems 95.'Human Robot Interaction and Cooperative Robots', Proceedings. 1995 IEEE/RSJ International Conference on*, volume 1, pages 399–406. IEEE, 1995.

[13] Kyoungchul Kong, Joonbum Bae, and Masayoshi Tomizuka. Control of rotary series elastic actuator for ideal force-mode actuation in human–robot interaction applications. *IEEE/ASME Transactions on Mechatronics*, 14(1):105–118, 2009.

[14] Kirby Ann Witte, Juanjuan Zhang, Rachel W Jackson, and Steven H Collins. Design of two lightweight, high-bandwidth torque-controlled ankle exoskeletons. In *Robotics and Automation (ICRA), 2015 IEEE International Conference on*, pages 1223–1228. IEEE, 2015.

[15] Nikolaus Hansen. The cma evolution strategy: A tutorial. *arXiv preprint arXiv:1604.00772*, 2016.

[16] Jessica C Selinger and J Maxwell Donelan. Estimating instantaneous energetic cost during non-steady-state gait. *Journal of Applied Physiology*, 117(11):1406–1415, 2014.

[17] JM Brockway. Derivation of formulae used to calculate energy expenditure in man. *Human nutrition. Clinical nutrition*, 41(6):463–471, 1987.

[18] John A Nelder and Roger Mead. A simplex method for function minimization. *The computer journal*, 7(4):308–313, 1965.